Supplementary material

Water-rich conditions during titania atomic layer deposition in the 100°C-300°C temperature window produce films with Ti^{IV} oxidation state but large H and O content variations

Bingbing Xia[1], Jean-Jacques Ganem[1], Ian Vickridge[1], Emrick Briand[1], Sébastien Steydli[1], Rabah Benbalagh[2] and François Rochet[2]

1.Sorbonne Université, CNRS, Institut des NanoSciences de Paris (UMR 7588), SAFIR, 75005 Paris, France

2. Sorbonne Université, CNRS, Laboratoire de Chimie Physique, Matière et Rayonnement (UMR 7614), 75005 Paris, France

Corresponding author. Rochet François: francois.rochet@sorbonne-universite.fr; Jean-Jacques Ganem: Jean-Jacques.Ganem@insp.jussieu.fr; Ian Vickridge : ian.vickridge@insp.jussieu.fr

S1. C 1s core-levels

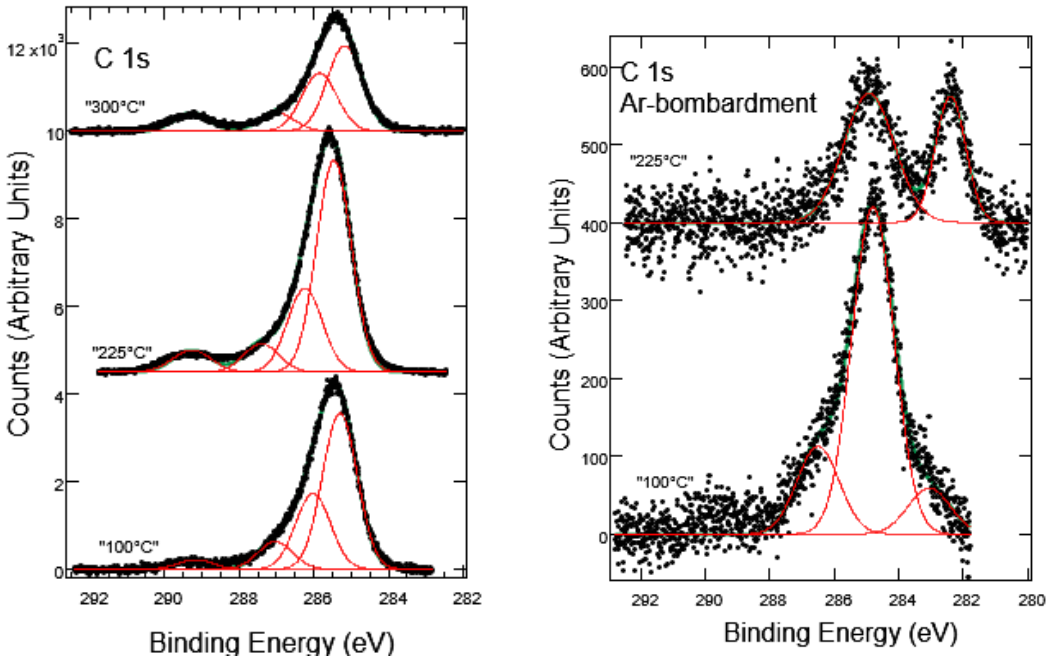

Figure S1. *Left panel: C 1s spectra recorded at normal photoelectron exit angle (hν=1487.1 eV) for the films produced at 100°C, at 225 °C, and 300°C. A Shirley background is subtracted. Right panel: Effect of the Ar bombardment (1 keV, 10^{-5} mbar, 8 min). The C 1s spectrum is fitted with sum of Gaussians (FWHM=1.15 eV). The peak at 289.3 eV is characteristic of the COO unit of carboxylic acids and esters.*

Sample	$\frac{I_{C\,1s}}{I_{Ti\,2p}}$
100°C	0.149
100°C plus Argon	0.024
225°C	0.203
225°C plus Argon	0.007
300°C	0.079

Table S1*. The* $\frac{I_{C\,1s}}{I_{Ti\,2p}}$ *ratio as a function of growth temperature and Ar-bombardment*

We consider the argon-sputtered 225°C film for which a large part of carbon contamination is eliminated. We can make two simplifying assumptions. First we assume that C atoms are

found only at the surface (the C carbon content in the bulk is zero). As C is detected by XPS this means that the cleaning is not complete. We can also assume that C atoms are evenly distributed from the surface to the depth. With this second assumption we can estimate an *upper bound value* of C concentration in the film.

The XPS intensity of core-level a X distributed evenly in depth is given by the following equation:

$$I_X = K \times T_{X\,Level}(KE) \times n_X \times \sigma_{X\,Level}(h\nu) \times \lambda_{X\,Level}(KE) \quad (1)$$

where K is a geometric constant, $T_{X\,Level}(KE)$ the transmission factor of the hemispherical analyzer (working at a given pass energy) for photoelectrons of kinetic energy KE, $\sigma_{X\,Level}(h\nu)$ the photoionization cross-section at excitation energy hν, and $\lambda_{X\,Level}(KE)$ the inelastic mean free path of photoelectrons of kinetic energy KE. n_X is the number of atoms X per unit volume.

The knowledge of $\frac{I_{C\,1s}}{I_{Ti\,2p}}$ gives $\left(\frac{n_C}{n_{Ti}}\right)^{XPS}$ through

$$\left(\frac{n_C}{n_{Ti}}\right)^{XPS} = \frac{I_{C\,1s}}{I_{Ti\,2p}} \times \frac{\sigma_{Ti\,2p}}{\sigma_{C\,1s}} \times \frac{\lambda_{Ti\,2p}}{\lambda_{C\,1s}} \times \frac{T_{Ti\,2p}}{T_{C\,1s}} \quad (2)$$

$\left(\frac{n_C}{n_{Ti}}\right)^{XPS}$ contains the transmission factors of the photoelectrons, which depend on the kinetic energy KE. T(KE) varies typically as KE^{-m} with m~0.5.[1] Therefore $\frac{T_{Ti\,2p}}{T_{C\,1s}} \approx \left(\frac{1027}{1201}\right)^{-0.5}$ that is 1.08, close to 1. Thus, we will neglect changes in the transmission factor and we will calculate:

$$\left(\frac{n_C}{n_{Ti}}\right)^{XPS} \approx \frac{I_{C\,1s}}{I_{Ti\,2p}} \times \frac{\sigma_{Ti\,2p}}{\sigma_{C\,1s}} \times \frac{\lambda_{Ti\,2p}}{\lambda_{C\,1s}} \quad (2)$$

that is:

$$\left(\frac{n_C}{n_{Ti}}\right)^{XPS} \approx 0.007 \times \frac{0.1069}{0.01367} \times \frac{22.00}{24.80} = 0.048$$

Therefore, considering a TiO_2 stoichiometry, an upper bound estimate of C content is 1.6 at% in the Ar-sputtered 225°C film.

S2. O 1s core-level

The O 1s spectra are shown in Figure S2. The main component at ~530.5 eV is attributed to O^{2-} bulk ions (O_{3c}). However, there is a "tail" at higher binding energy that is represented by two Gaussians at ~531.6 eV (ΔBE=1.1 eV with respect to O^{2-}main peak) and ~532.7 eV (ΔBE=2.2 eV). This tail is attributed to hydroxyls (OH).[2],[3],[4],[5],[6] These hydroxyls can be incorporated during the film growth. Indeed, formed after the H_2O step, some Ti-OH bonds may not react during the successive TDMAT half-cycle. Hydroxyls can also form at the surface as the film is exposed to water (last cycle) and exposed to air before being introduced in the XPS setup. On the clean anatase (101) surface water breaks into H^+ and HO^- species (23% of the adsorbed molecules according to an XPS study[4]). H^+ adsorbs on an O_{2c} site forming a bridging OH, while HO^- binds to a Ti_{5c}^{4+} site, forming a terminal OH. The O 1s BE of hydroxyls and molecular water on (101) anatase were calculated by Patrick et al..[5] O_{3c} and surface O_{2c} oxygens contribute to a peak at 530.2 eV. The terminal OH is found at 531.3 eV (ΔBE=1.1 eV from the main O^{2-} peak), and the bridging OH at 532.0 eV (ΔBE=1.8 eV). Therefore, the O 1s components found at ΔBE =1.1 eV and 2.2 eV in the experimental spectra could be attributed to hydroxyl groups. The calculated O 1s ΔBE of molecular water sitting on a Ti_{5c}^{4+} site of anatase is 3.8 eV when it is isolated from the co-adsorbed OHs, reduced to 3.1 eV when molecular water makes a H donor bond with a nearby OH. Therefore, we do not find evidence for molecular water adsorbed on the surface.

The attribution of the high BE O 1s components *only* in terms of hydroxyls must be considered with a *caveat*. For instance, Saari et al. [7] consider that they can be attributed to

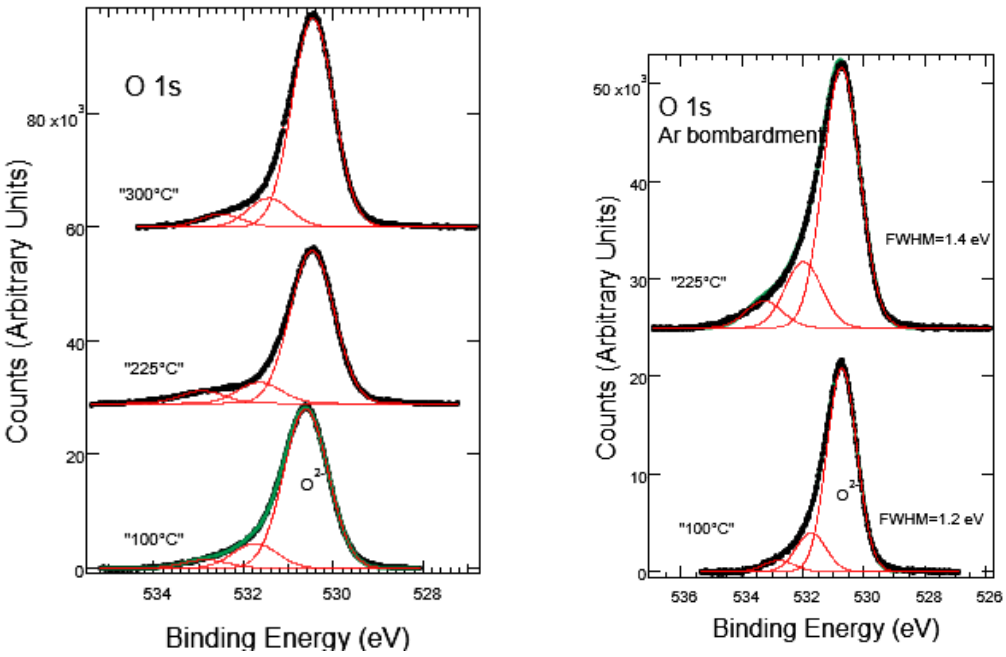

Figure S2. *Left panel: O 1s spectra recorded at normal photoelectron exit angle (hν=1487.1 eV) for the films produced at 100°C, 225 °C, and 300°C. A Shirley background is subtracted. The O 1s spectra are fitted with sums of Gaussians (FWHM=1.1 eV). Right panel: effect of the Ar bombardment (1 keV, 10^{-5} mbar, 8 min). The FWHM is indicated.*

100°C	100°C plus Ar	225°C	225°C plus Ar	300°C
530.61 (82.6)	530.72 (80.2)	530.47 (82.1)	530.72 (73.2)	530.46 (83.4)
531.74 (12.9)	531.73 (15.3)	531.64 (11.2)	531.96 (20.1)	531.43 (11.5)
532.83 (4.4)	532.79 (4.5)	532.91 (6.7)	533.38 (6.7)	532.51 (5.1)

Table S2. *Decomposition of the O 1s spectra (Figure S2) into three components. Binding energies (in eV) and weights (%) are given.*

peroxo interstitials. Moreover, from the C 1s spectra (Figure S1) we know that carbon-containing species are adsorbed on the surface. They can result from an incomplete reaction of TDMAT with H_2O, but as the samples are transported in air, carbon species can also adsorb on the sample surface, in particular alcohols and carboxylic acids. Indeed, the C 1s spectrum shows

a clear peak at 289.3 eV in the C 1s spectrum that is due to a carboxylic COOH unit or an ester.[8],[9] Unfortunately, these oxygen-containing carbon compounds also produce peaks in the 531.6-533.0 eV energy interval, and thus complexify the interpretation of the experimental O 1s spectra. The O 1s component of an alcohol is found at ~532.8 eV, the two inequivalent oxygen atoms components of aliphatic carboxylic acids are at 531.96 and 533.24 eV, and those of aromatic carboxylic acids are at 531.62 and 533.06 eV.[10] It should also be noticed that the component at 531.6 eV could be related to O vacancies.[11],[12] In fact, this component increases after the Ar-bombardment that induces O losses and the reduction of Ti^{4+} to Ti^{3+} and Ti^{2+} (Figure S4).

S3. O/Ti atomic ratios with XPS

We consider that O and Ti are evenly distributed in depth. Then the O 1s intensity $I_{O\ 1s}$ and the Ti 2p spectrum intensity $I_{Ti\ 2p}$ are given by equation (1). From $\frac{I_{O\ 1s}}{I_{Ti\ 2p}}$ we can now calculate the ratio $\left(\frac{n_O}{n_{Ti}}\right)^{XPS}$ where n_O and n_{Ti} are the number of oxygen atoms and titanium atoms per unit volume, respectively:

$$\left(\frac{n_O}{n_{Ti}}\right)^{XPS} = \frac{I_{O\ 1s}}{I_{Ti\ 2p}} \times \frac{\sigma_{Ti\ 2p}}{\sigma_{O\ 1s}} \times \frac{\lambda_{Ti\ 2p}}{\lambda_{O\ 1s}} \times \frac{T_{Ti\ 2p}}{T_{O\ 1s}} \quad (3)$$

$\frac{T_{Ti\ 2p}}{T_{O\ 1s}} \approx \left(\frac{1027}{956}\right)^{-0.5}$ is 0.97, i.e. close to 1. Neglecting changes in the transmission factor, we obtain:

$$\left(\frac{n_O}{n_{Ti}}\right)^{XPS} \approx \frac{I_{O\ 1s}}{I_{Ti\ 2p}} \times \frac{\sigma_{Ti\ 2p}}{\sigma_{O\ 1s}} \times \frac{\lambda_{Ti\ 2p}}{\lambda_{O\ 1s}} \quad (4)$$

$\left(\frac{n_O}{n_{Ti}}\right)^{XPS}$ values are given in Table S2.

We first consider the "as-grown" (not sputtered) samples. Taking the whole O 1s intensity, we get $\left(\frac{n_O}{n_{Ti}}\right)^{XPS}$ in the 2.33 to 2.48 range for the films grown in the 100°C-300°C range. However, if we consider only the bulk O^{2-} intensity and eliminate the high BE components of dubious assignment (due to contamination), then $\left(\frac{n_O}{n_{Ti}}\right)^{XPS}$ is close to 2 (1.95-2.03).

It is also very instructive to notice that the Ar bombardment leads to a heavy loss of oxygen in agreement with the observation of the Ti^{3+} and Ti^{2+} oxidation states in the Ti 2p spectra (see Figure S5).

Sample	$\frac{I_{O\ 1s}(total)}{I_{Ti\ 2p}}$	$\left(\frac{n_O}{n_{Ti}}\right)^{XPS}$ (Total O)	$\frac{I_{O\ 1s}(O^{2-})}{I_{Ti\ 2p}}$	$\left(\frac{n_O}{n_{Ti}}\right)^{XPS}$ (only O^{2-})
100 °C	0.868	2.45	0.717	2.02
100°C plus Ar	0.807	2.27	-	1.82
225°C	0.879	2.48	0.721	2.03
225°C plus Ar	0.744	2.10	-	1.53
300°C	0.827	2.33	0.690	1.95

Table S3*. Ti 2p normalized O 1s intensities(* $\frac{I_{O\ 1s}(total)}{I_{Ti\ 2p}}$ *and* $\frac{I_{O\ 1s}(O^{2-})}{I_{Ti\ 2p}}$*) and calculated ratios* $\left(\frac{n_O}{n_{Ti}}\right)^{XPS}$

S4. N 1s spectra: quantitative aspects

The kinetic energies of the Ti 2p (1027 eV) and N 1s (1086 eV) photoelectrons are very close, therefore the transmission factor ratio $\frac{T_{Ti\ 2p}}{T_{N\ 1s}}$ is close to 1 (we can estimate that $\frac{T_{Ti\ 2p}}{T_{N\ 1s}} \approx$

$\left(\frac{1027}{1086}\right)^{-0.5} = 1.03$). Therefore, assuming that all nitrogen species are located at the oxide surface, we can estimate the equivalent nitrogen surface density N_N^{XPS} by considering that

$$I_{N\ 1s} = K \times T_{N\ 1s}(KE) \times N_N^{XPS} \times \sigma_{N\ 1s}(h\nu) \quad (5)$$

and that

$$I_{Ti\ 2p} = K \times \alpha \times T_{Ti\ 2p}(KE) \times n_{Ti\ 2p} \times \sigma_{Ti\ 2p}(h\nu) \times \lambda_{Ti\ 2p}(KE) \quad (6)$$

where α is a coefficient (<1) accounting for the attenuation of Ti 2p signal by the top layer of nitrogen species. Then we get:

$$N_N^{XPS} \approx \frac{I_{N\ 1s}}{I_{Ti\ 2p}} \times \frac{\sigma_{Ti\ 2p}}{\sigma_{N\ 1s}} \times \frac{T_{Ti\ 2p}}{T_{N\ 1s}} \times \alpha \times \lambda_{Ti\ 2p} \times n_{Ti}^{anatase} \quad (7)$$

Sample	$\frac{I_{N\ 1s}}{I_{Ti\ 2p}}$	N_N^{XPS} (10^{14} cm^{-2})
100°C	0.0219	6.3
100°C plus Ar	0.0094	-
225°C	0.0197	5.6
225°C plus Ar	0.0025	-
300°C	0.0069	2.0

Table S4. $\frac{I_{N\ 1s}}{I_{Ti\ 2p}}$ *as a function of sample growth temperature and/or treatment.* N_N^{XPS} *values are calculated considering a constant transmission factor and the density of anatase.*

When the nitrogen content is below one monolayer (ML or ~10^{15} atoms/cm^3) α ~1. N_N^{XPS} values calculated in the limit of α=1 are collected in Table S4 (we take $\frac{T_{Ti\ 2p}}{T_{N\ 1s}} \approx 1$ and $n_{Ti}^{anatase}$, i.e.

2.98×10^{22} cm^{-3}). The nitrogen surface density is indeed in the 10^{14} cm^{-2} range, validating the estimation of α.

S5. N 1s spectra of the Ar bombarded "100°C" and "225°C" samples

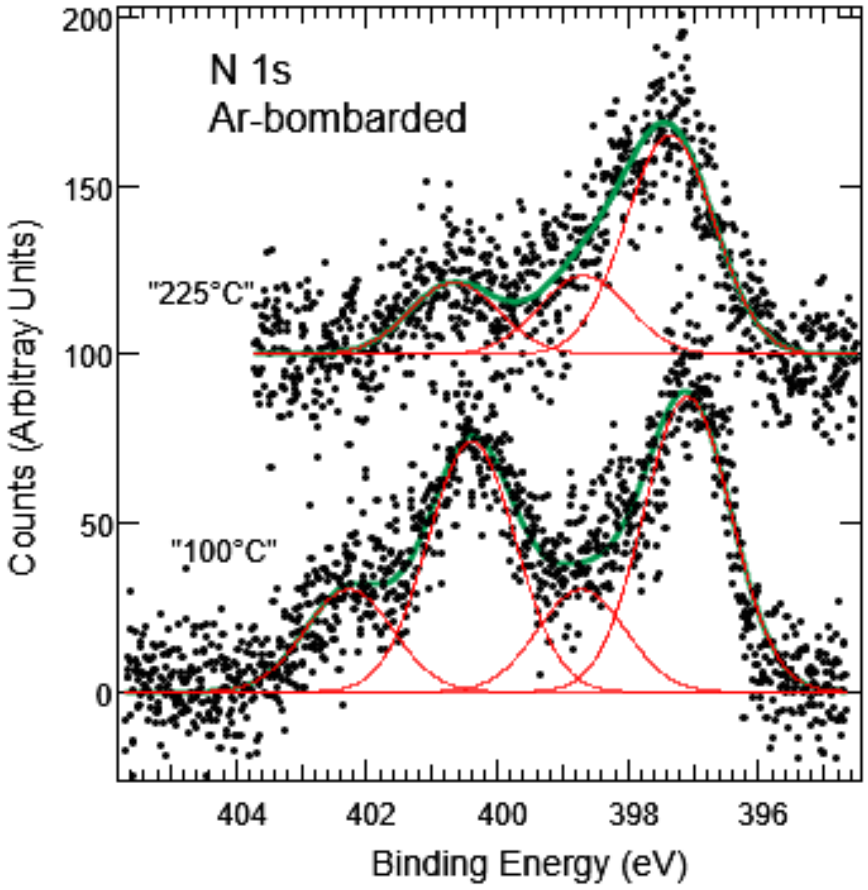

Figure S3. *N 1s spectra of the Ar-bombarded "100°C" and "225°C" samples (1 keV, 10^{-5} mbar, 8 min). A Shirley background is subtracted. Note the appearance of a component at 397.1-397.3 eV due to the decomposition of the DMA molecule under the ion beam.*

Concerning the N 1s spectrum (Figure S6, Table S5), the sputtering leads to a strong decrease of N 1s signal. For the "100°C" sample, the $\frac{I_{N\ 1s}}{I_{Ti\ 2p}}$ ratio decreases from 2×10^{-2} to 10^{-2}. For the

sputtered “225°C”, the $\frac{I_{N\ 1s}}{I_{Ti\ 2p}}$ ratio decreases from 2×10^{-2} to 2×10^{-3} (Table S3). In both cases, the Ar bombardment leads to the decomposition of the adsorbed molecules, as a fourth component in the ~397.1 eV-397.3 eV range shows up. This can be attributed to the decomposition of DMA and formation of an adsorbed nitrile.[13]

100°C plus Ar BE (eV)	225°C plus Ar
402.27 (13.7)	-
400.40 (33.4)	400.65 (19.5)
398.71 (13.7)	398.68 (21.3)
397.10 (33.4)	397.36 (59.2)

Table S5. *BE and weight (%) of the fitting components of N 1s spectra in Figure S6.*

S6. VBE determination

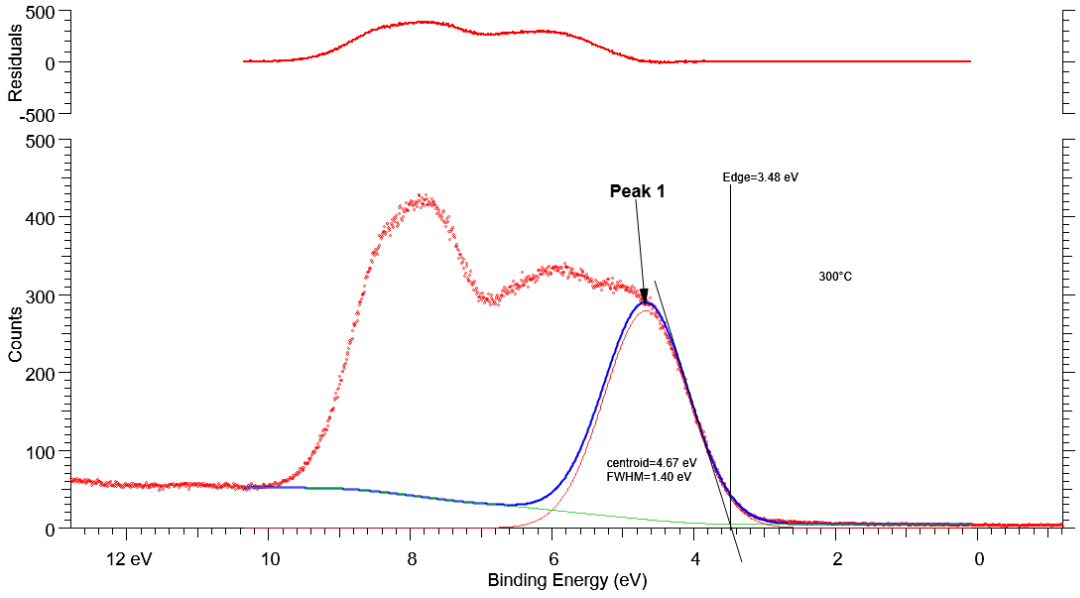

Figure S4. *Determination of the valence band edge (VBE).*

We first calculate the background (green line) and then position a Gaussian function that best reproduces the O 2p edge. The binding energy of the valence band edge (VBE) is determined as the intersection of the tangent at the Gaussian inflexion point with the x-axis using the equation:[14]

$$\mathrm{BE(VBE)} = \mathrm{E(centroid)} - \frac{\mathrm{FWHM}}{\sqrt{2\ln(2)}} = \mathrm{E(centroid)} - 0.849 \times \mathrm{FWHM} \quad (8)$$

S7. Ti 2p and valence band of the Ar-bombarded "100°C" and "225°C" films

Ar-bombardment cannot be carried out to make a composition profile of the titania layers. Already after eliminating a few surface monolayers, with Ar-bombardment (1 keV, 10^{-5} mbar, 8 min) O losses induce a reduction of the sample. Indeed, we observe substantial amounts of Ti^{3+} and Ti^{2+} in the Ti 2p spectrum of the bombarded amorphous "100°C" and anatase "225°C" samples (Figure S5). Concomitantly, the density of shallow gap states in the valence band, that extends from the Fermi level down to ~0.4 eV below,[15] is sufficient to form a Fermi edge (Figure S6).

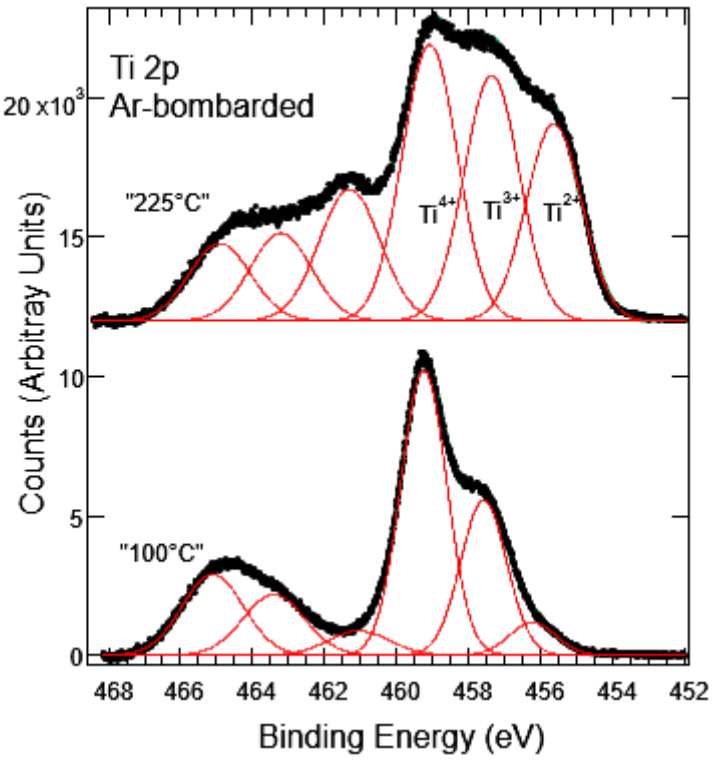

Figure S5. *Ti 2p spectra of the Ar-bombarded "100°C" and "225°C" samples (1 keV, 10^{-5} mbar, 8 min). A Shirley background is subtracted. The fitting components are Gaussians of FWHM 1.5 eV and 2 eV for the Ti $2p_{3/2}$ and Ti $2p_{1/2}$ levels respectively.*

Oxidation state	100°C plus Ar BE (eV)	225°C plus Ar BE (eV)
Ti^{4+}	459.25 (60.3)	459.08 (38.0)
Ti^{3+}	457.58 (32.7)	457.36 (34.0)
Ti^{2+}	456.23 (7.0)	455.53 (28.0)

Table S6. *BE and weight (%) of the fitting components of Ti $2p_{3/2}$ in Figure S4.*

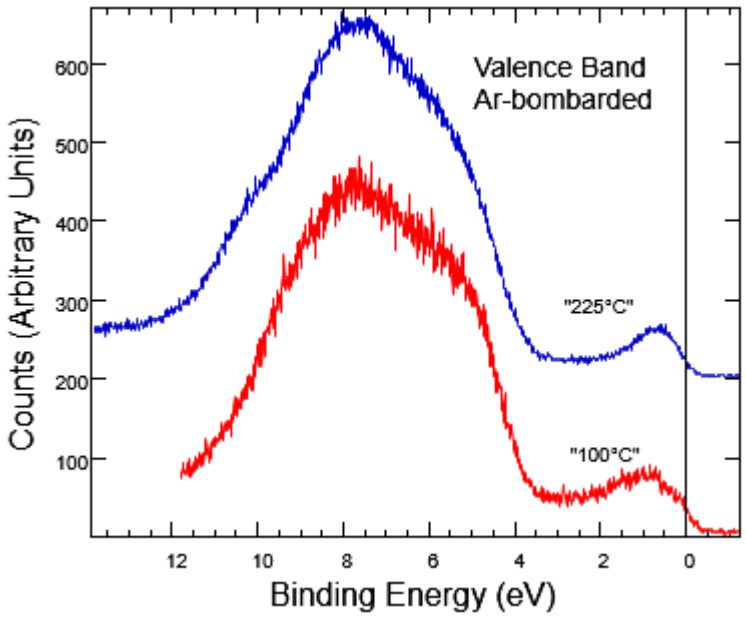

Figure S6. *Valence band spectra of the Ar-bombarded "100°C" and "225°C" samples (1 keV, 10^{-5} mbar, 8 min). No background is subtracted. The vertical line marks the position of the Fermi level.*

References

[1] P. Jiříček, Measurement of the transmission function of the hemispherical energy analyser of ADES 400 electron spectrometer, Czechoslov. J. Phys. 44 (1994) 261–267. https://doi.org/10.1007/BF01694490.

[2] G. Martra, Lewis acid and base sites at the surface of microcrystalline TiO2 anatase: relationships between surface morphology and chemical behaviour, Appl. Catal. A Gen. 200 (2000) 275–285. https://doi.org/10.1016/S0926-860X(00)00641-4.

[3] G. Ketteler, S. Yamamoto, H. Bluhm, K. Andersson, D.E. Starr, D.F. Ogletree, H. Ogasawara, A. Nilsson, M. Salmeron, The Nature of Water Nucleation Sites on TiO2(110) Surfaces Revealed by Ambient Pressure X-ray Photoelectron Spectroscopy, J. Phys. Chem. C. 111 (2007) 8278–8282. https://doi.org/10.1021/jp068606i.

[4] L.E. Walle, A. Borg, E.M.J. Johansson, S. Plogmaker, H. Rensmo, P. Uvdal, A. Sandell, Mixed Dissociative and Molecular Water Adsorption on Anatase TiO 2 (101), J. Phys. Chem. C. 115 (2011) 9545–9550. https://doi.org/10.1021/jp111335w.

[5] C.E. Patrick, F. Giustino, Structure of a Water Monolayer on the Anatase TiO2 (101) Surface, Phys. Rev. Appl. 2 (2014) 014001. https://doi.org/10.1103/PhysRevApplied.2.014001.

[6] Z. Futera, N.J. English, Exploring Rutile (110) and Anatase (101) TiO 2 Water Interfaces by Reactive Force-Field Simulations, J. Phys. Chem. C. 121 (2017) 6701–6711. https://doi.org/10.1021/acs.jpcc.6b12803.

[7] J. Saari, H. Ali-Löytty, M.M. Kauppinen, M. Hannula, R. Khan, K. Lahtonen, L. Palmolahti, A. Tukiainen, H. Grönbeck, N. V. Tkachenko, M. Valden, Tunable Ti 3+ -Mediated Charge Carrier Dynamics of Atomic Layer Deposition-Grown Amorphous TiO 2, J. Phys. Chem. C. (2022) acs.jpcc.1c10919. https://doi.org/10.1021/acs.jpcc.1c10919.

[8] F. Bournel, J.-J. Gallet, U. Köhler, B.B. Ellakhmissi, S. Kubsky, S. Carniato, F. Rochet, Propanoate grafting on (H,OH)-Si(0 0 1)-2 × 1, J. Phys. Condens. Matter. 27 (2015) 054005. https://doi.org/10.1088/0953-8984/27/5/054005.

[9] D. Briggs, G. Beamson, Primary and secondary oxygen-induced C1s binding energy shifts in x-ray photoelectron spectroscopy of polymers, Anal. Chem. 64 (1992) 1729–1736. https://doi.org/10.1021/ac00039a018.

[10] D. Briggs, G. Beamson, XPS studies of the oxygen 1s and 2s levels in a wide range of functional polymers, Anal. Chem. 65 (1993) 1517–1523. https://doi.org/10.1021/ac00059a006.

[11] W. Göpel, J.. Anderson, D. Frankel, M. Jaehnig, K. Phillips, J.. Schäfer, G. Rocker, Surface defects of TiO2(110): A combined XPS, XAES AND ELS study, Surf. Sci. 139 (1984) 333–346. https://doi.org/10.1016/0039-6028(84)90054-2.

[12] M. Takeuchi, Y. Onozaki, Y. Matsumura, H. Uchida, T. Kuji, Photoinduced hydrophilicity of TiO2 thin film modified by Ar ion beam irradiation, Nucl. Instruments Methods Phys. Res. Sect. B Beam Interact. with Mater. Atoms. 206 (2003) 259–263. https://doi.org/10.1016/S0168-583X(03)00736-5.

[13] A. Zakhtser, A. Naitabdi, R. Benbalagh, F. Rochet, C. Salzemann, C. Petit, S. Giorgio,

Chemical Evolution of Pt–Zn Nanoalloys Dressed in Oleylamine, ACS Nano. 0 (2020) null-null. https://doi.org/10.1021/acsnano.0c03366.

[14] L. Pérez Ramírez, A. Boucly, F. Saudrais, F. Bournel, J.-J. Gallet, E. Maisonhaute, A.R. Milosavljević, C. Nicolas, F. Rochet, The Fermi level as an energy reference in liquid jet X-ray photoelectron spectroscopy studies of aqueous solutions, Phys. Chem. Chem. Phys. 23 (2021) 16224–16233. https://doi.org/10.1039/D1CP01511G.

[15] P. Reckers, M. Dimamay, J. Klett, S. Trost, K. Zilberberg, T. Riedl, B.A. Parkinson, J. Brötz, W. Jaegermann, T. Mayer, Deep and Shallow TiO 2 Gap States on Cleaved Anatase Single Crystal (101) Surfaces, Nanocrystalline Anatase Films, and ALD Titania Ante and Post Annealing, J. Phys. Chem. C. 119 (2015) 9890–9898. https://doi.org/10.1021/acs.jpcc.5b01264.